https://ntrs.nasa.gov/search.jsp?R=19690005585 2020-03-12T08:28:23+00:00Z

N/X

Report No. 03-68-84

N 69 14917
NASA CR 98718

J-72821

Quarterly Report No. 2

LITHIUM-DIFFUSED SOLAR CELLS

October 1968

For the Period
1 July 1968 – 30 September 1968

Contract No. 952248

Prepared by

Don L. Kendall
Raymond A. Vineyard

Texas Instruments Incorporated
P.O. Box 5012
Dallas, Texas 75222

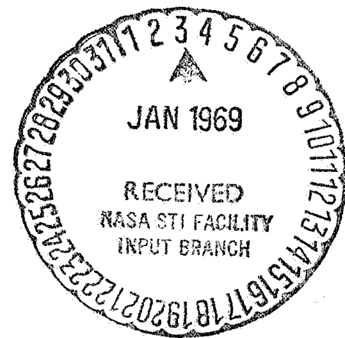

for

Jet Propulsion Laboratory
California Institute of Technology
4800 Oak Grove Avenue
Pasadena, California

Report No. 03-68-84

Quarterly Report No.2

LITHIUM-DIFFUSED SOLAR CELLS

October 1968

For the Period
1 July 1968 – 30 September 1968

Contract No. 952248

Prepared by:

Don L. Kendall
Raymond A. Vineyard

Texas Instruments Incorporated
P.O. Box 5012
Dallas, Texas 75222

for

Jet Propulsion Laboratory
California Institute of Technology

As Sponsored by:

The National Aeronautics and Space Administration
Under Contract NAS7-100

This work was performed for the Jet Propulsion Laboratory, California Institute of Technology, as sponsored by the National Aeronautics and Space Administration under Contract NAS7-100.

TECHNICAL CONTENT

This material contains information prepared by Texas Instruments Incorporated under JPL Subcontract. Its content is not necessarily endorsed by the Jet Propulsion Laboratory, California Institute of Technology, or The National Aeronautics and Space Administration.

ABSTRACT

Lithium is generally observed, in silicon as an interstitial donor. However, lithium substitutional acceptors have been identified and their concentrations measured. Heavily boron-doped silicon ($5 \times 10^{19} cm^{-3}$) has been compensated by lithium and the resultant resistivity (apparent) determined as a function of time. Solar cells were fabricated from Lopex* and Float-zoned silicon by the standard evaporated Li source technique followed by a 400°C diffusion for 90 minutes on each group.

* Trademark of Texas Instruments Incorporated

TABLE OF CONTENTS

SECTION	TITLE	PAGE
I.	INTRODUCTION	1
II.	SUBSTITUTIONAL LITHIUM	2
III.	LITHIUM COMPENSATION OF BORON DOPED SILICON	4
IV.	CELL FABRICATION	6
V.	WORK PLANNED	7
VI.	NEW TECHNOLOGY	8
VII.	REFERENCES	9

LIST OF ILLUSTRATIONS

FIGURE	TITLE	PAGE
1.	Silicon Box, Longitudinal Section	10
2.	Silicon Box, Exploded View	10
3.	Apparent Resistivity versus Time	11
4.	Resistivity versus Time	11

SECTION I

INTRODUCTION

The objective of the contract is to conduct a program to determine process parameter effects upon lithium-diffused, silicon solar cell electrical and mechanical characteristics.

SECTION II

SUBSTITUTIONAL LITHIUM

The lithium species generally observed in silicon is an interstitial donor. However, from a thermodynamic standpoint there must also be some finite concentration of a substitutional lithium species which would be expected to be acceptor, defined as Li_{Si} when ionized. As an example of this type of behavior, Li in GaAs can be either an interstitial donor or a substitutional acceptor.[1] The donor form is dominant in heavily P-type GaAs and the acceptor form dominates in heavily N-type GaAs. The identification of Li_{Si} could be important to theoretical understanding of the annealing processes observed in silicon solar cells following electron irradiation.[2]

To test for such a species in silicon we have diffused lithium into heavily N-type silicon (phosphorus doped) and observed the change in resistivity and electron mobility. The substitutional lithium concentration should be enhanced by the factor n/n_i, where n is the free electron concentration (which is essentially the phosphorus concentration) and n_i is the intrinsic electron concentration at the diffusion temperature. For a temperature of 1000°C, n_i is 8×10^{18} cm^{-3}. So, for a phosphorus concentration of 5.5×10^{19} cm^{-3} the enhancement factor, n/n_i, is about 7. The interstitial donor form of lithium should be *depressed* by a similar factor. This simple treatment is not precise because of the high solubility of the lithium in otherwise undoped silicon. This is about 5×10^{19} cm^{-3} at 1000°C, which exceeds n_i and complicates the analysis somewhat. Nevertheless, the same principles apply, and we should be able to make some reasonable estimate of the lithium substitutional concentration at 1000°C from the observed change in carrier concentration in heavily phosphorus-doped silicon. Similar data at other diffusion temperatures should allow estimates to be made of the feasibility of the formation of substitutional lithium following an irradiation event, for example by the reaction:

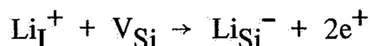

$$Li_I^+ + V_{Si} \rightarrow Li_{Si}^- + 2e^+$$

The data for sequential lithium diffusions at 1000°C are shown in Table I. The repeated diffusions were necessary to avoid depleting the lithium sources. This occurred by oxidation primarily and was made evident after about one hour of diffusion at 1000°C by the attendant decrease in the sample resistivity (after an initial increase).

The diffusion scheme that finally evolved consisted of a "silicon box" approach reminiscent of that used by Miller and Savage[3] for aluminum diffusion into silicon. This is shown in Figures 1 and 2. The lithium was applied to the carrier slices by evaporation. The lithium first permeates the carrier slices and then crosses the boundary to the sample to be diffused. The samples were quenched in liquid nitrogen following diffusion.

The data in Table I show that the average resistivity increases by a factor of 2.7 and the effective mobility shows no significant change. If the latter had *increased* significantly, an ion-pairing mechanism between the lithium acceptors and phosphorus donors would have been indicated, since this would have reduced the concentration of ionized scattering centers. However, since it did not change we must assume that the primary effect is the introduction of lithium substitutional acceptors, Li_{Si}^-. The concentration of acceptors added is about 3.5×10^{19} cm^{-3}.

Control runs on companion phosphorus-doped samples showed no change in resistivity on heating at 1000°C for periods of several hours.

From the above estimate of the substitutional lithium concentration in heavily phosphorus-doped silicon, we can reverse the solubility enhancement arguments discussed earlier and estimate the substitutional lithium concentration in silicon containing only lithium to be about 1/7 of that in the phosphorus-doped case. Thus, the concentration of Li_{Si}^- in silicon doped to the solubility limit at 1000°C is about 5×10^{18} cm^{-3}, which represents about 10% of the total lithium in the sample at this temperature.

SECTION III

LITHIUM COMPENSATION OF BORON DOPED SILICON

Using the same diffusion method outlined in the previous section, heavily boron-doped silicon (5×10^{19} cm^{-3}) has been compensated by lithium. Reiss and Fuller[4] have previously observed lithium-boron compensation, although they reported no electrical measurements on the compensated material. We have achieved apparently very exact compensation with four-point probe readings of apparent resistivity made immediately after the 30 minute lithium diffusion ranging from 10^4 Ω-cm to 5×10^5 Ω-cm. The apparent resistivity is defined from the geometry of a four-point probe with 10-mil probe spacing to be:

$$\rho = 2\pi s \frac{V}{I} = 0.16 \frac{V}{I} (\Omega\text{-cm})$$

Where s is the probe spacing, V is the voltage across the two inner probes, and I is the current between two outer probes. In other words, no attempt has been made to correct for thickness of the material being measured.

Readings of apparent resistivity, however, vary with time. After seeming to increase slightly for 3 to 5 minutes, they fall one order of magnitude in 30 minutes and another order of magnitude in 24 hours. Figure 3 is a plot of apparent resistivity versus time for two samples which represent approximately the upper and lower limits of initial resistivity observed. Figure 4 extends the lower curve out to 65 hours after diffusion. Samples which initially are indicated as N-type on a thermoelectric probe change to P-type in the same 3 to 5 minute period that the apparent resistivity seems to rise.

This effect appears to be entirely a surface effect, since lapping the surface on which measurements are being taken will restore the apparent resistivity to the same value observed just after the lithium diffusion. The amount of lapping necessary (approximately 1 mil) to restore the high resistivity is considerably more than can be explained by out diffusion of lithium to the surface of the material, although this is still the primary suspect as the mechanism involved.

Whether the lithium diffuses to surfaces created by lapping damage or the out-diffusion is somehow enhanced by the presence of boron is unknown, but is clear that a p-type surface skin develops on the n-type bulk of the samples. The formations of this layer precludes analysis of the electrical properties of the heavily compensated bulk since the P/N junction, as well as the comparitively low resistance of the surface, cause current from measurement equipment to flow through the skin and not the bulk.

Hall measurements on these samples reflect the behavior described above, but the apparent carrier concentration and mobility are not meaningful in absence of information on junction depth progression with time.

SECTION IV

CELL FABRICATION

Lots 3 and 4 were fabricated from Lopex* and Float-zoned silicon, respectively. The lots were processed identically with a 90 minute lithium-diffusion at 400°C and a 3 minute contact sinter at 600°C. Sixty cells from each lot were identified, measured electrically, and shipped to JPL. The electrical characteristics of the cells in lots 3 and 4 are shown in Tables II and III. The light source was filtered tungsten at an intensity of 100 mW/cm^2 equivalent sunlight and was calibrated with n or p solar cells. The data are presented for comparison pruposes under a fixed spectral distribution and should not be necessarily interpreted as absolute.

* Trademark of Texas Instruments Incorporated

SECTION V

WORK PLANNED

The absolute efficiency of lithium-diffused cells will be established under the filtered-xenon solar simulator recently installed at TI. Lot 4 will be fabricated to yield a uniform Li-profile across the entire slice. Out-diffusion at the edges and non-uniform profiles due to incomplete Li coverage of the slice will be eliminated by processing a whole, round slice through contact sintering. Two cells will then be sawed from each slice and antireflective coated. Lot 6 will be manufactured by the standard Li-evaporation process with a 325°C diffusion for 8 hours. Work will continue on the tin-lithium diffusion technique.

SECTION VI

NEW TECHNOLOGY

No reportable items of new technology have been identified during this report period.

SECTION VII

REFERENCES

1. Don L. Kendall, *Semiconductors and Semi-Metals*, (R. K. Willardson and Albert C. Beer, eds.) Vol. 4, p.234.

2. J. J. Wysocki, P. Rappaport, E. Davison, and R. Hand, *Appl. Phys. Letters*, 9, 44 (1966).

3. R. C. Miller and A. J. Savage, *J. Appl. Physics*, 27, 1430 (1956).

4. H. Reiss and C. H. Fuller, *Trans. AIME*, J206, 276 (1956).

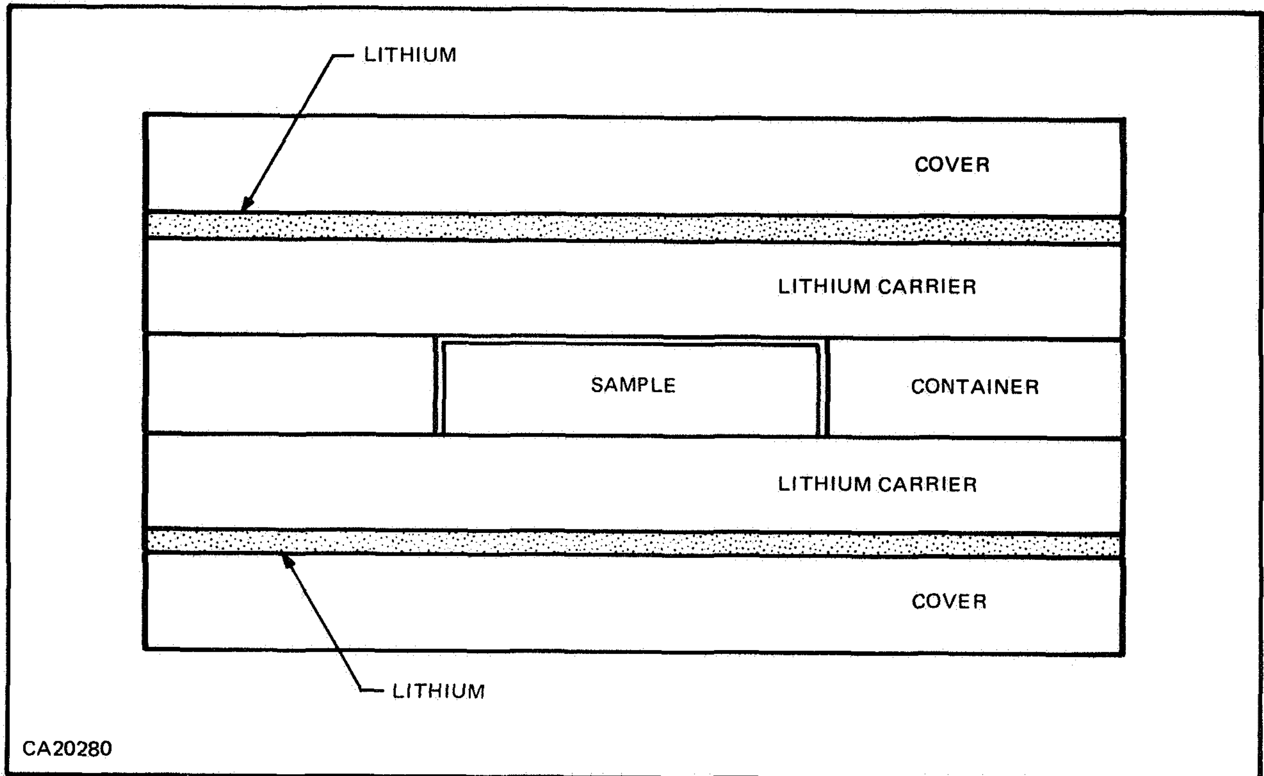

Figure 1. Silicon Box, Longitudinal Section

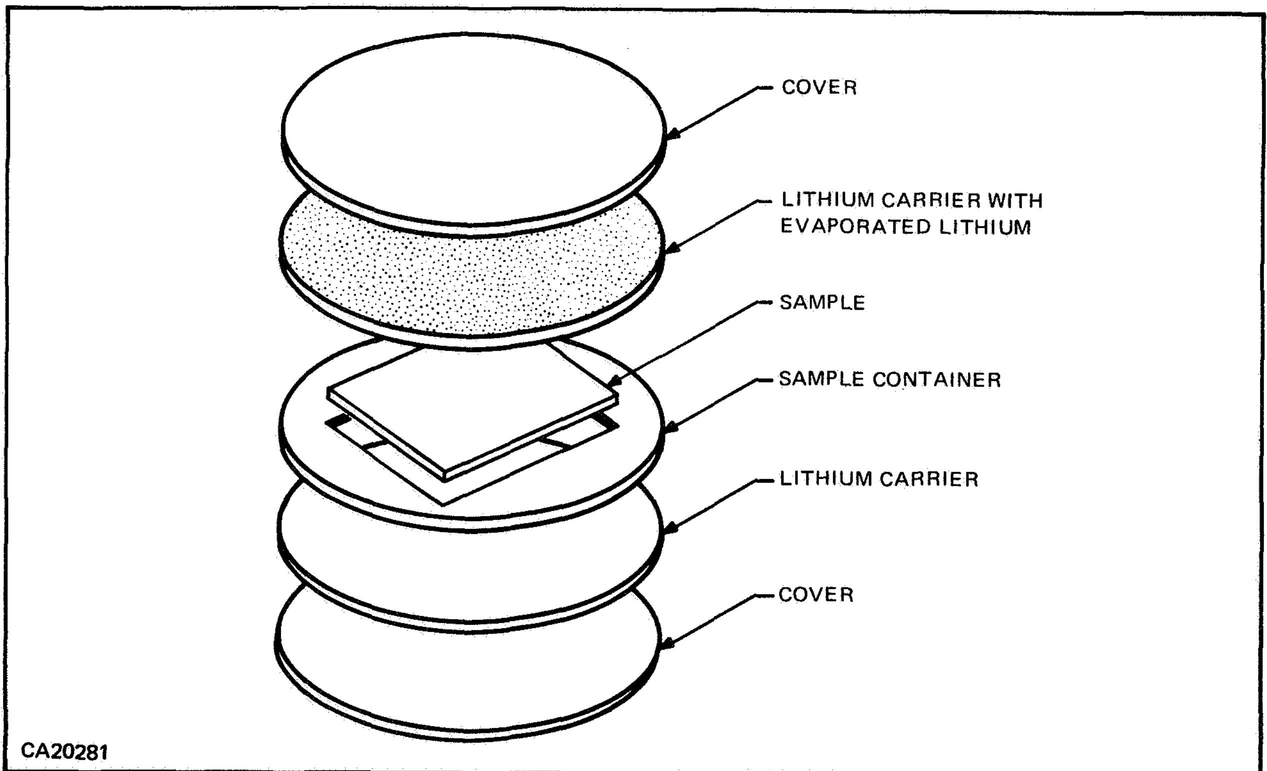

Figure 2. Silicon Box, Exploded View

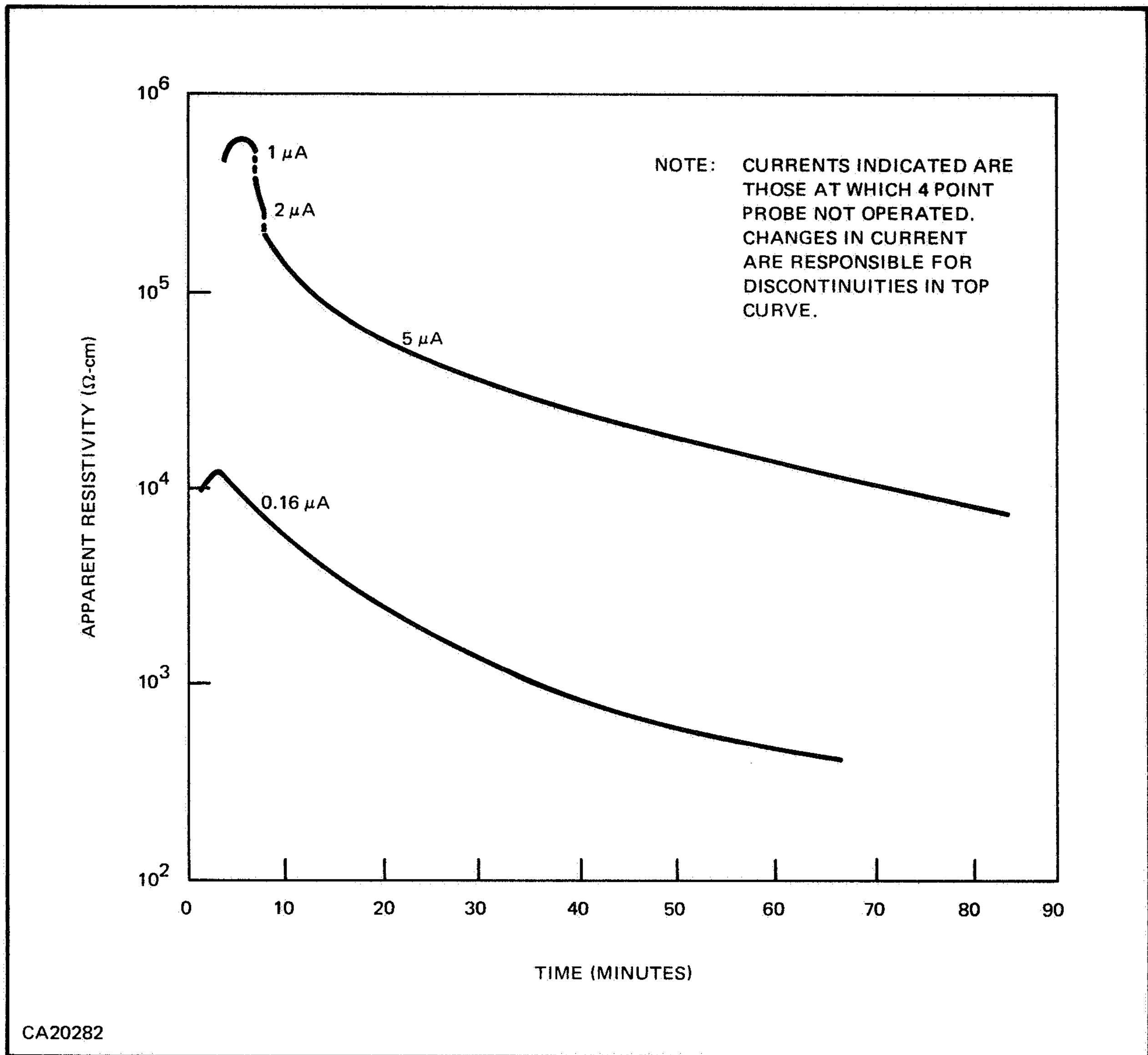

Figure 3. Apparent Resistivity versus Time

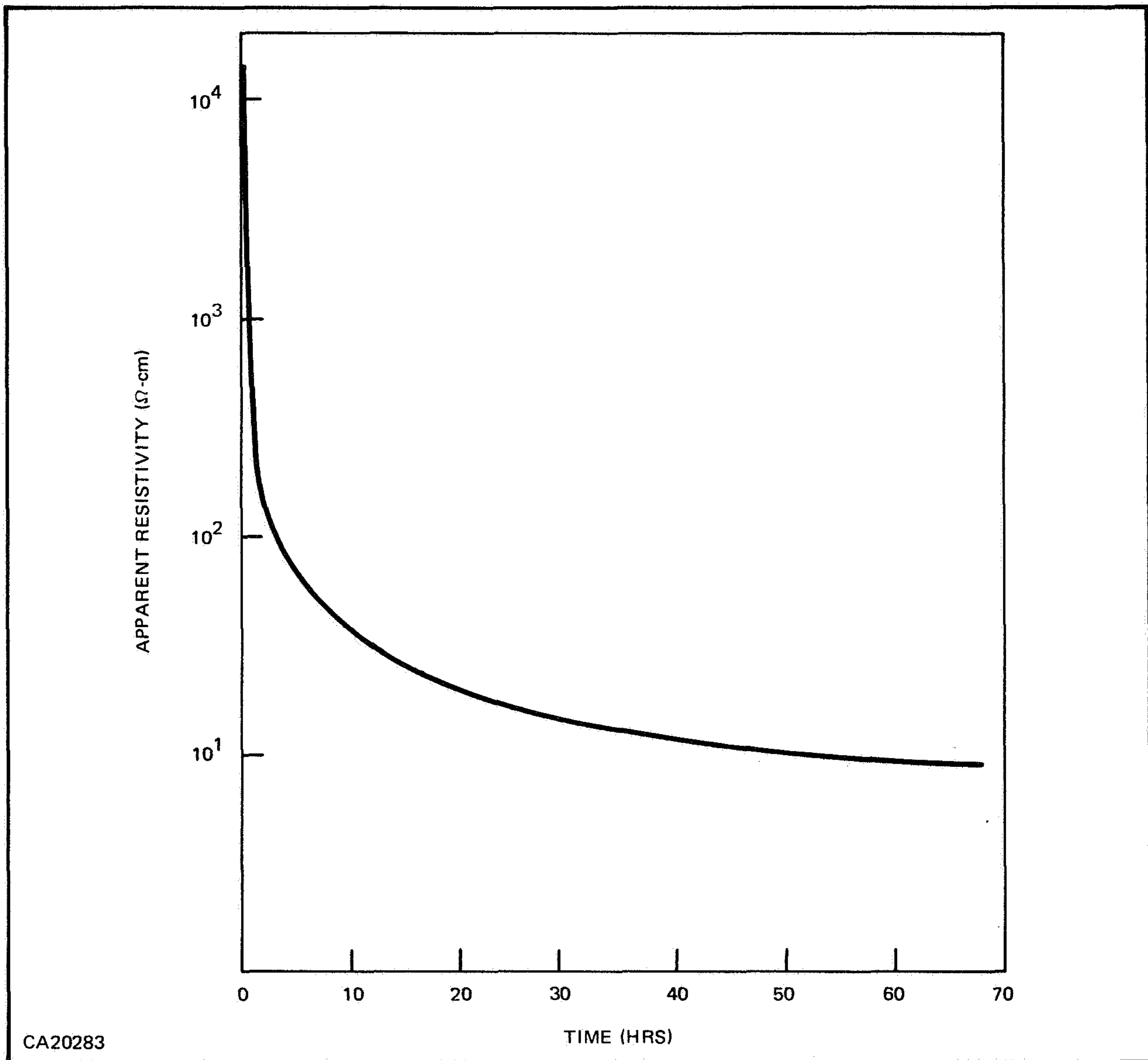

Figure 4. Resistivity versus Time

Table I. Sample Resistivity, Mobility, and Carrier Concentration Versus Lithium Diffusion Time*

Cumulative Diffusion Time (MIN)	Resistivity (Ω-cm)	Carrier Conc. (cm^{-3})	Mobility (cm^2 $volt^{-1}$ sec^{-1})
0	1.68×10^{-3}	5.4×10^{19}	69
30	1.79×10^{-3}	5.4×10^{19}	66
65	1.94×10^{-3}	4.7×10^{19}	68
90	2.35×10^{-3}	3.9×10^{19}	69
120	3.05×10^{-3}	3.2×10^{19}	64
150	3.62×10^{-3}	3.0×10^{19}	64
270	4.49×10^{-3}	1.9×10^{19}	71

*Times include time for Lithium to penetrate carrier slices (see Text and Figures 1 and 2).

Table II. Cell Characteristics of Lot 3
(90 Minute Diffusion at 400°C into Lopex* Silicon)

Cell No. (T3)	I_{SC} (mA)	$I_{0.430\ V}$ (mA)	Voc (V)	Cell No. (T3)	I_{SC} (mA)	$I_{0.430\ V}$ (mA)	Voc (V)
1	58.2	55.0	0.595	31	56.5	50.0	0.580
2	56.8	53.0	0.590	32	57.8	50.0	0.590
3	57.8	54.0	0.592	33	55.5	50.0	0.590
4	57.0	53.0	0.590	34	56.9	52.0	0.590
5	56.8	53.0	0.595	35	54.8	50.5	0.588
6	57.0	53.8	0.590	36	56.5	48.8	0.578
7	57.2	52.6	0.590	37	58.1	55.8	0.595
8	56.0	53.0	0.595	38	59.5	55.8	0.595
9	55.8	51.6	0.592	39	58.5	56.0	0.600
10	57.3	52.5	0.585	40	59.0	55.9	0.598
11	57.9	53.0	0.588	41	58.8	54.0	0.590
12	56.5	52.8	0.590	42	58.2	54.2	0.599
13	56.5	53.0	0.593	43	58.5	55.0	0.599
14	56.8	53.1	0.592	44	59.2	54.8	0.590
15	57.0	51.0	0.574	45	58.8	53.8	0.590
16	56.0	50.9	0.590	46	58.5	53.3	0.590
17	56.1	52.1	0.590	47	58.0	53.0	0.590
18	56.8	51.0	0.588	48	58.9	54.1	0.590
19	57.8	51.5	0.580	49	59.6	53.0	0.590
20	58.3	51.5	0.580	50	57.5	52.4	0.590
21	57.2	51.4	0.580	51	58.6	53.0	0.590
22	55.0	51.2	0.592	52	58.5	51.0	0.578
23	56.0	50.8	0.588	53	57.5	51.5	0.585
24	54.5	50.0	0.588	54	59.0	52.5	0.585
25	57.0	49.0	0.572	55	57.0	53.6	0.590
26	55.1	49.9	0.590	56	57.5	53.9	0.593
27	54.5	50.0	0.589	57	56.5	52.2	0.590
28	57.0	50.6	0.582	58	55.0	52.0	0.595
29	53.5	49.5	0.580	59	56.0	51.9	0.590
30	57.8	51.2	0.589	60	57.5	51.5	0.590
Avg.	57.1	52.3	0.589				
Low	53.5	48.8	0.572				
High	59.5	56.0	0.600				

* Texas Instruments Incorporated Registered Trademark

Table III. Cell Characteristics of Lot 4
(90 Minute Diffusion at 400°C into FZ Silicon)

Cell No. (T4)	I_{SC} (mA)	$I_{0.430\ V}$ (mA)	Voc (V)	Cell No. (T4)	I_{SC} (mA)	$I_{0.430\ V}$ (mA)	Voc (V)
1	53.9	51.1	0.590	31	52.6	48.0	0.590
2	54.2	51.3	0.591	32	52.7	48.0	0.590
3	55.6	51.0	0.583	33	53.7	48.7	0.585
4	53.0	49.9	0.587	34	53.0	48.2	0.582
5	54.0	49.0	0.587	35	53.8	49.5	0.588
6	53.5	50.3	0.589	36	53.7	48.5	0.582
7	54.0	50.0	0.585	37	51.8	47.9	0.588
8	54.0	50.0	0.590	38	53.8	48.0	0.590
9	54.0	50.6	0.590	39	52.9	48.0	0.582
10	55.0	49.9	0.588	40	53.0	48.0	0.580
11	52.0	49.2	0.590	41	53.2	48.0	0.582
12	52.6	49.8	0.590	42	52.0	47.8	0.580
13	52.0	49.8	0.589	43	52.1	48.5	0.588
14	53.0	49.9	0.584	44	54.0	48.9	0.588
15	52.8	49.9	0.590	45	53.6	48.2	0.580
16	53.0	50.0	0.589	46	52.0	48.5	0.590
17	54.0	49.5	0.585	47	52.2	47.8	0.590
18	52.3	48.3	0.590	48	52.0	47.0	0.590
19	52.5	49.0	0.588	49	52.5	47.2	0.582
20	54.0	50.0	0.583	50	51.8	47.5	0.588
21	54.6	49.5	0.582	51	52.5	46.1	0.580
22	54.0	49.7	0.585	52	52.0	47.6	0.580
23	53.2	49.0	0.588	53	51.8	47.8	0.582
24	53.8	49.0	0.590	54	50.0	47.5	0.590
25	53.2	49.5	0.585	55	51.9	47.0	0.587
26	52.5	49.2	0.590	56	52.8	47.8	0.580
27	51.7	48.8	0.590	57	53.0	47.0	0.580
28	52.0	47.5	0.585	58	54.8	48.0	0.588
29	52.1	48.0	0.585	59	53.0	47.5	0.585
30	53.0	48.2	0.580	60	52.8	47.5	0.582
Avg.	53.0	48.8	0.586				
Low	50.0	46.1	0.580				
High	55.6	51.3	0.591				